

Processing Doppler Lidar and Cloud Radar Observations for Analysis of Convective Mass Flux Parameterizations Using DYNAMO Direct Observations

R. Michael Hardesty
CIRES/University of Colorado/NOAA
325 Broadway
Boulder, Colorado 80305
phone: (303) 497-6568 fax: (303) 497-5318 email: mike.hardesty@noaa.gov

Award Number: N00014-13-1-0897
<http://cires.colorado.edu>

LONG-TERM GOALS

This work is being done in conjunction with other observational and modelling research aimed at improving the representation of the Madden-Julian Oscillation (MJO) in global models. It combines remote sensing and in-situ observations made from the RV-Revell during legs 2 & 3 of the DYNAMO experiment to help characterize vertical transport through the boundary layer and to build statistics of the vertical extent and propagation speed of precipitation driven outflows that passed over the ship.

OBJECTIVES

The connection between convection and environmental moisture and evolution of cloud processes is of significant scientific interest. The question of whether cumulus clouds provide a local moistening of the troposphere above the cloudy boundary layer, or if the moistening is due to a larger-scale mechanism for moisture convergence that facilitates the growth of the moist layer? The focus of this research effort was to compute mass flux from remote sensing data obtained during DYNAMO, and to investigate whether cold pools that emanate from convection organize the interplay between humidity and convection and hence play a role in the moistening of the upper troposphere.

APPROACH

Our approach is to analyze HRDL observations obtained during DYNAMO in combination with observations from the shipboard cloud radar under weakly or non-precipitating conditions to calculate mass flux, and to combine those estimates with estimates of surface fluxes, and to develop new analysis tools to determine phase speed and depth of precipitation-driven outflows in order to investigate the role of convective activity strength on outflow characteristics. The team included the Principal Investigator along with Dr. Alan Brewer and Dr. Aditya Choukulkar.

WORK COMPLETED

In order to characterize the mass flux transport occurring during the DYNAMO field campaign the data gathered from the High Resolution Doppler Lidar (HRDL) and the 94-GHz cloud Doppler radar

(W-band radar) were combined. To accomplish this, first the clear air velocity signal was de-convolved from the Doppler velocity measured by the W-band radar using the Pinsky et al. (2010) approach. The details of this approach are explained in the Results section. The clear air retrievals were validated against HRDL measurements using the data from VOCALS (Variability of the American Monsoon Systems' (VAMOS) Ocean-Cloud-Atmosphere-Land Study) campaign. Future work will involve using this method to perform retrievals on the W-band data from the DYNAMO dataset.

Using the HRDL data, the updraft/downdraft structure during the MJO2 (Oct 4th to Oct 30th) event was studied. From this the updraft fraction and convective mass flux velocity were calculated (Lappen and Randall, 2001). These measured values of the updraft fraction and convective mass flux were compared to the parameterized values using the parameterization proposed by Randall et al. (1992). Comparisons were made for the different stages of the MJO2 event. It was observed that the mass flux parameterization agrees with observations at lower altitudes while the parameterization for updraft fraction agrees with observations at higher altitudes. Future work will investigate the effect of different averaging time to see if there are any improvements in the comparison. In addition, the modifications to the parameterization scheme presented in Lappen and Randall (2001) will also be studied.

The HRDL scanning data were used to track the leading edge of precipitation driven outflows as they propagated within 10 km of the ship. Outflow boundaries could typically be identified in both the radial wind speed and aerosol backscatter intensity fields. HRDL's 20 minute repeating scan sequence included two nearly horizontal (1 degree elevation) azimuthal scans once roughly every 10 minutes and a pattern of shallow (0-30 degree) elevation scans oriented in along two orthogonal azimuthal angles. Taking about 30 seconds per sweep, there were three elevation scans along each azimuth angle and the entire pattern was repeated every twenty minutes. Common features in the outflow boundaries were manually selected in the horizontal scans for repeated sweeps and used to track the absolute position of the boundary through time. The depth of the outflow was determined using vertical scans of the radial wind speed and aerosol backscatter strength. The position of the outflow boundary in time was used to estimate the propagation speed and direction of each outflow.

RESULTS

Retrieval of Clear Air Velocities from W-band Radar

Two of the products measured by a vertically pointing Doppler radar are the radar reflectivity, $Z(h,t)$ and the vertical velocity $V(h,t)$. The vertical velocity measured by the Doppler radar is the sum of the clear air velocity $W(h,t)$ and the sedimentation or fall velocity of the precipitation $V_g(h,t)$.

$$V(h,t) = W(h,t) + V_g(h,t) \quad (1)$$

Where h is the vertical height coordinate and t is the time.

In order to de-convolve the clear air velocity signal from the sedimentation velocity signal the Pinsky et al. (2010) approach is used. The above two components of the Doppler velocity can be further split into the mean and turbulent components as shown in Eq 2.

$$V(h,t) = W(h,t) + V_g(h,t) = \overline{W}(h,t) + W'(h,t) + \overline{V}_g(h,t) + V'_g(h,t) \quad (2)$$

The mean Doppler velocity is a strong function of the radar reflectivity given that both the sedimentation velocity and the radar reflectivity increase with drop size. The relationship between the measured Doppler velocity and the radar reflectivity at three levels is shown in Figure 1. Therefore for each height level a relationship between the sedimentation velocity and the radar reflectivity can be estimated as shown in Eq 3.

$$\langle V \rangle = \langle V_g \rangle = \varphi(\langle Z \rangle) \quad (3)$$

Using this function, it is possible to filter out the effect of the mean sedimentation velocity from the observed Doppler velocity. In addition, we assume that the mean clear air velocity is equal to zero. This leaves us with the following equation for the residual velocity

$$U(h,t) = V(h,t) - \varphi(h, \langle Z \rangle) = W'(h,t) + V'_g(h,t) \quad (4)$$

This residual velocity is still a function of the sedimentation velocity, due to the sedimentation velocity fluctuations being related to the variations of the drop size distributions within the clouds. That is the variance of the residual velocity depends on the reflectivity. The relationship between the variance of the residual velocity and radar reflectivity is shown in Figure 2 and can be expressed as:

$$W'(h,t) = a[Z(h,t)]U(h,t) \quad (5)$$

$$V'_g(h,t) = \{1 - a[Z(h,t)]\}U(h,t) \quad (6)$$

Where , $a(Z) = a_0 / \theta(Z)$ and $a_0 = \frac{\sum_{k=1}^N \theta^{-1}[Z(h,t_k)]}{\sum_{k=1}^N \theta^{-2}[Z(h,t_k)]}$

Validation:

In order to validate the Pinsky et al. (2010) retrieval technique, the clear air retrievals from the W-band radar are compared to the HRDL measured vertical velocities. For this comparison we use data from the VOCALS campaign. During the VOCALS campaign, the HRDL and W-band were operating in a similar manner as the DYNAMO campaign. In addition, during the VOCALS campaign there were several instances where there is overlapping data from both the W-band and HRDL. The W-band retrieved clear air velocities and HRDL measured vertical velocities are shown in Figure 3. The vertical velocity statistics from the W-band and HRDL are presented in Figure 4.

Evaluation of Mass Flux Closure:

First order closure models the vertical fluxes in the following manner:

$$\overline{w'x'} = -K \frac{\partial X}{\partial z} \quad (7)$$

where x is the concentration of some atmospheric variable separated into mean (X) and turbulent (x') components. The limitation of this approach is that this parameterization does not allow modeling

counter-gradient fluxes that may occur during highly convective conditions (Lappen and Randall 2001). In order to overcome this limitation, a mass flux approach was proposed (Randall et al., 1992). Mass flux approach divides the atmosphere into updrafts and downdrafts such that:

$$X = \sigma_{up} X_{up} + \sigma_{dn} X_{dn} \quad (8)$$

where X_{up} and X_{dn} are the mean concentrations during updrafts and downdrafts respectively and σ_{up} and σ_{dn} are the updraft and downdraft fractions respectively.

And the fluxes are modeled as:

$$\overline{w'x'} = M_* (X_{up} - X_{dn}) \quad (9)$$

Where M_* is called the mass flux velocity and given by:

$$M_* = \sigma_{up} \times \sigma_{dn} (w_{up} - w_{dn}) \quad (10)$$

Mass flux parameterizations offer an inherently non-local approach. It captures the fluxes through estimation of the updraft/downdraft fractions (Eq 8) and mass flux velocity (Eq 10). To determine the updraft fraction and mass flux velocity, Randall et al. (1992) proposed a parameterization to determine these terms physically. These parameterizations are shown in Eq 11 and Eq 12.

$$\sigma = \frac{1}{2} - \frac{S_w}{2[4 + S_w^2]^{1/2}} \quad (11)$$

$$M_* = \left[\frac{\overline{w'^2}}{4 + S_w^2} \right]^{1/2} \quad (12)$$

Where S_w is the skewness of the clear air vertical velocity.

The DYNAMO dataset provides a unique opportunity where the measured values of the updraft fraction and the mass flux velocity can be compared to the parameterized values. In order to compare the parameterized values to measurements, the MJO 2 (Oct 4 to Oct 30, 2011) event was selected. The MJO2 event can be split into 3 regimes based on the net heat flux and cloud forcing data (shown in Figure 5): (1) Suppressed, (2) Disturbed and (3) MJO active.

A preliminary comparison of the measured versus parameterized quantities for the above regimes is shown in Figures 6 through 8. In general, it is observed that the parameterization for the mass flux velocity agrees with the measurement at heights lower than ~600 m and deviates at higher altitudes. The updraft fraction on the other hand, does not agree with measurement at lower altitudes (below ~600 m) and agrees well at higher altitudes (above ~600 m). The reason for this is as yet unclear. However, it is possible that the averaging time over which these statistics are estimated plays an important role. The results presented here are based on 10 minute averages. Future work will investigate the effect of longer averaging times. In addition, some modifications made to the parameterization scheme (Lappen and Randall 2001) will also be tested to see if these modifications show any improvement.

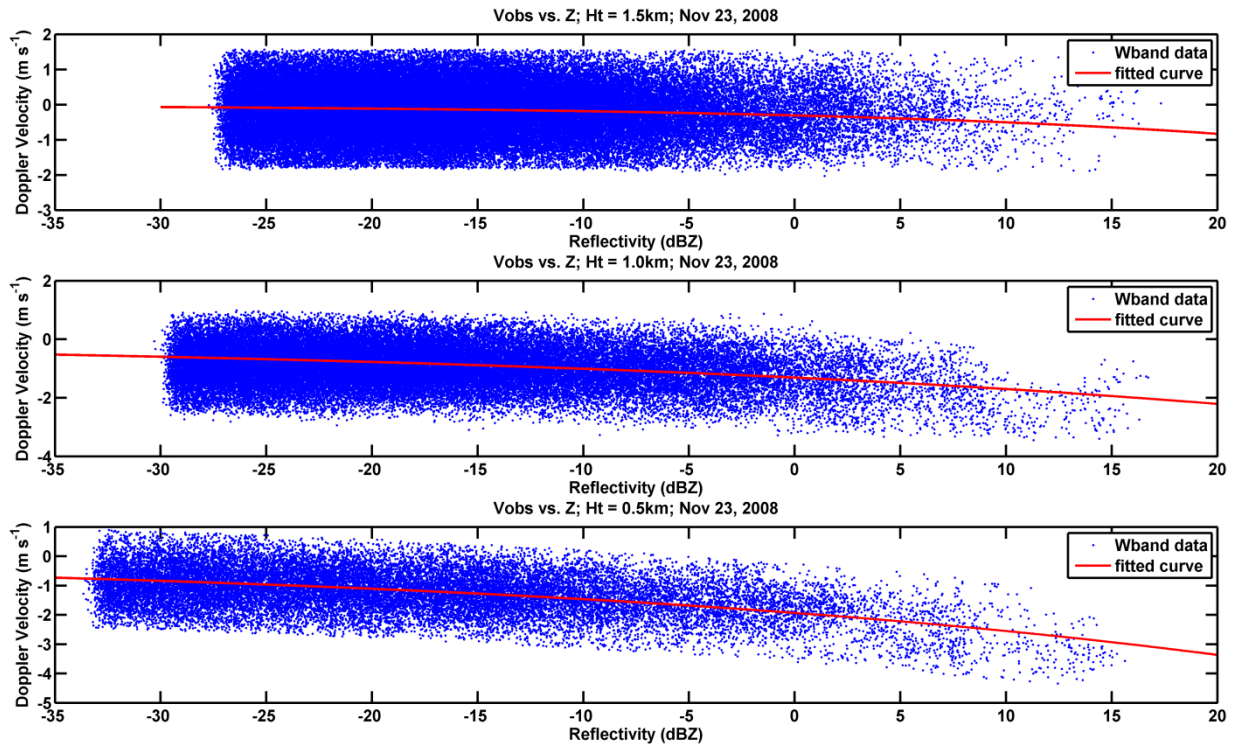


Figure 1. The relationship between the measured Doppler velocity and the radar reflectivity at 0.5 km, 1 km and 1.5 km above sea level.

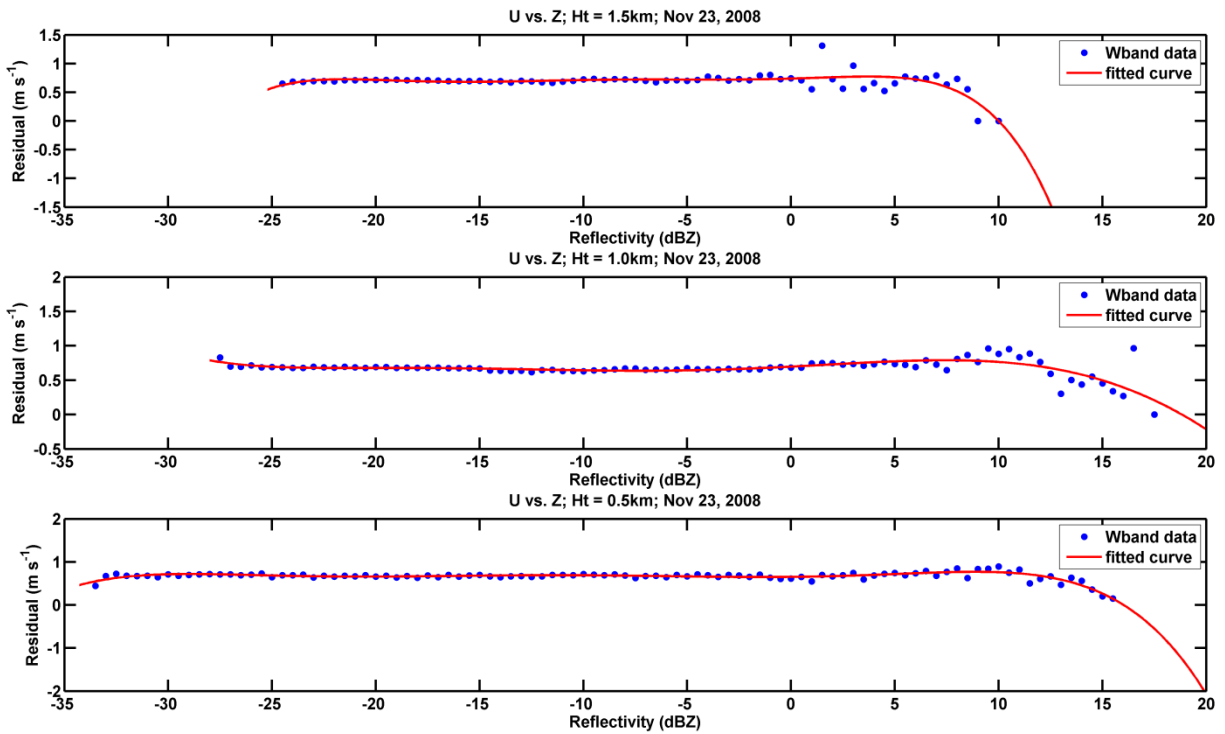


Figure 2. The relationship between the variance of the residual velocity and radar reflectivity at 0.5 km, 1 km and 1.5 km above sea level.

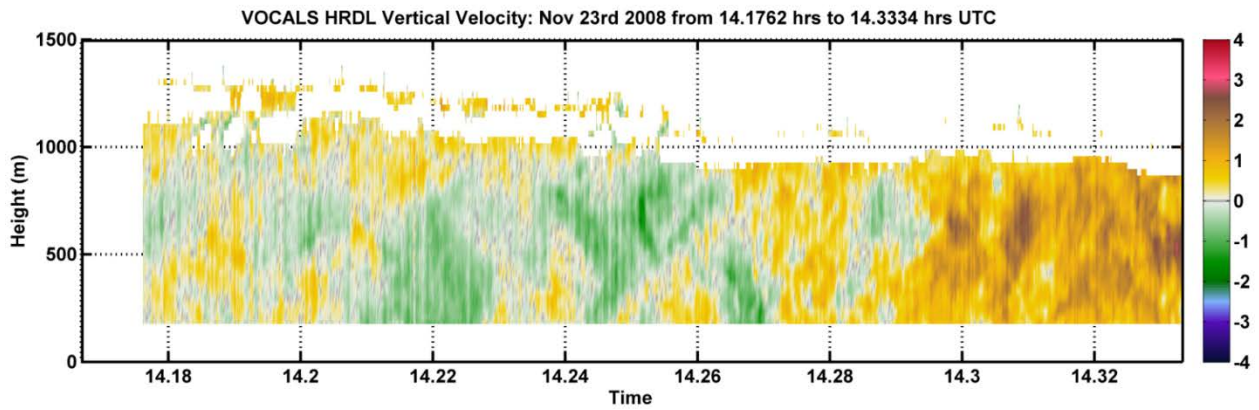
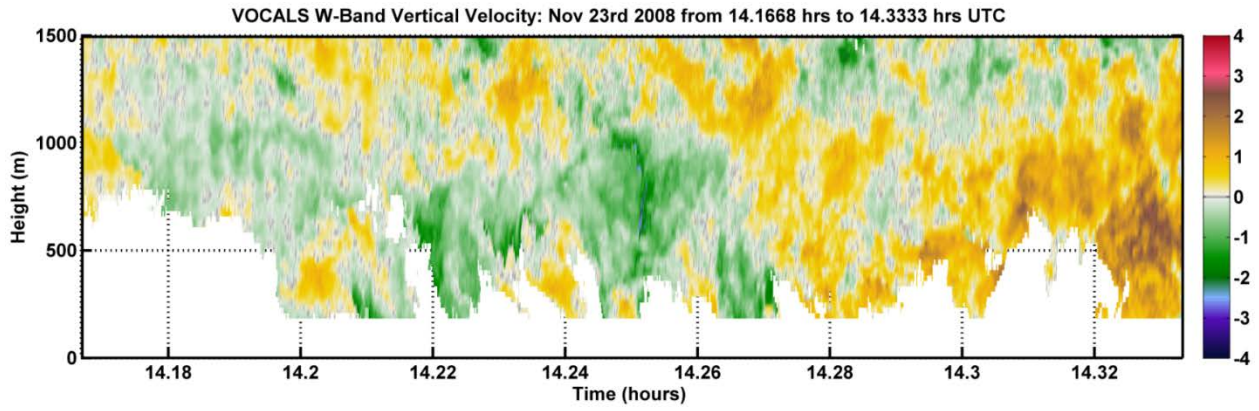


Figure 3: Comparison of W-band clear air retrievals with HRDL measurements

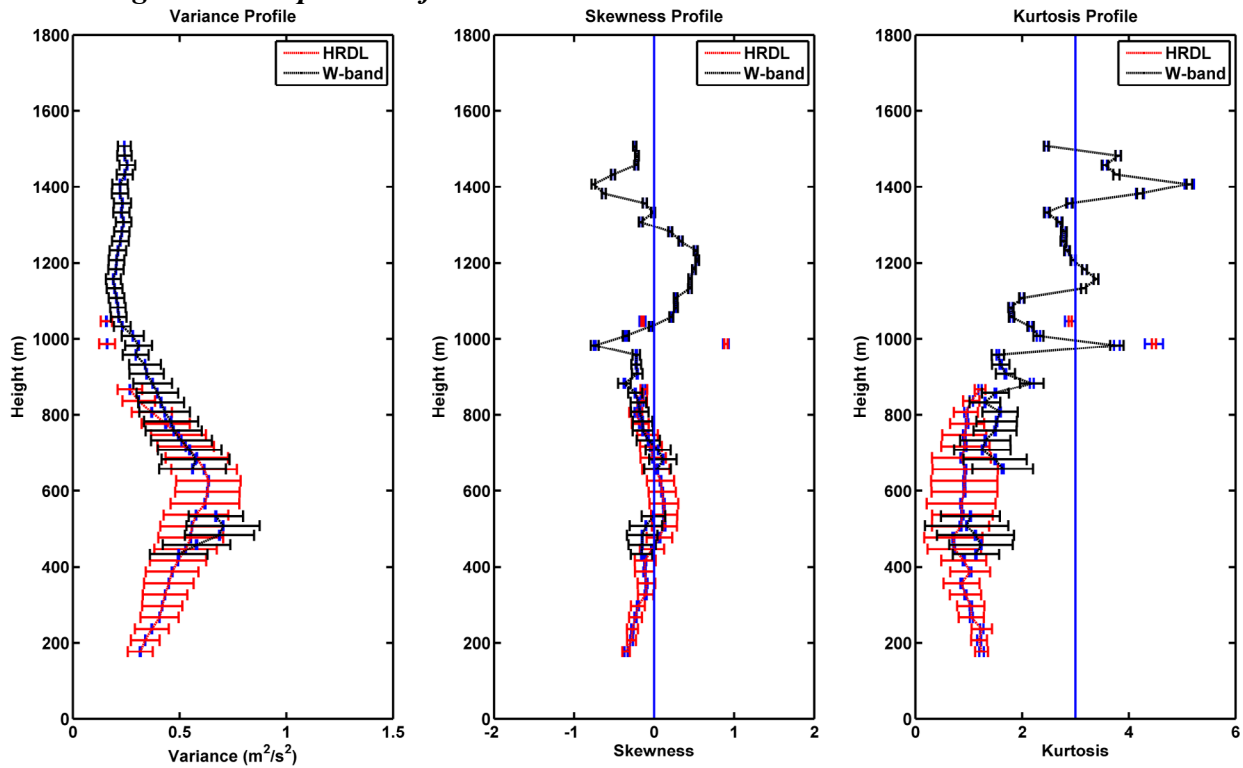


Figure 4: Comparison of W-band (black line) retrieved vertical velocity statistics with those retrieved from HRDL (red line).

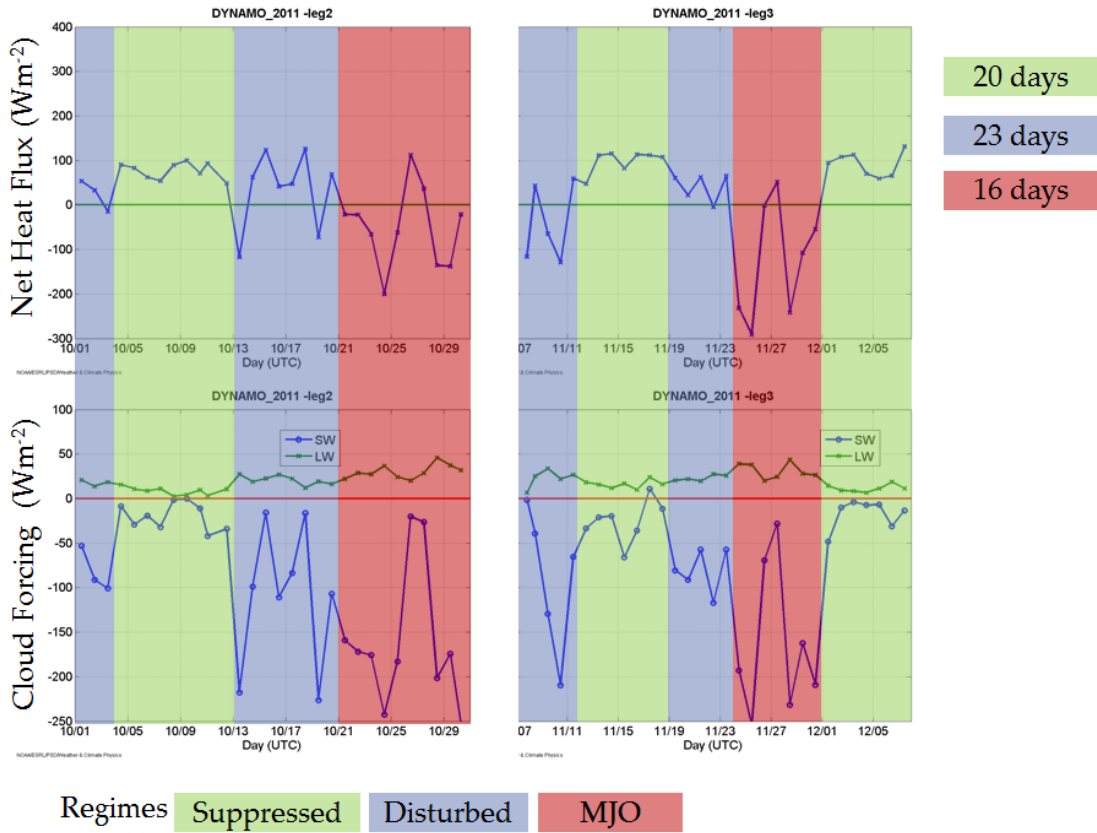


Figure 5. The different regimes observed during the DYNAMO campaign based on net heat flux and cloud forcing.

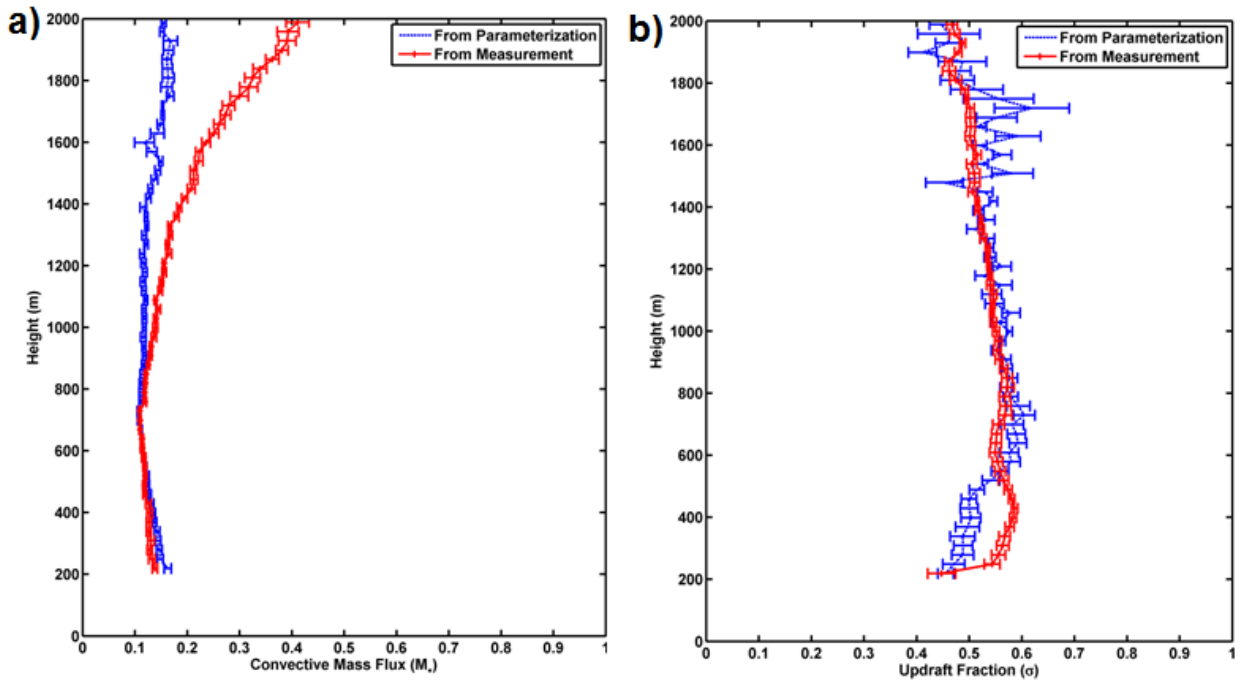


Figure 6: Comparison of parameterized (blue line) and measured values (red line) during the suppressed phase. (a) Convective mass flux and (b) Updraft fraction. The error bars indicate uncertainty in the estimate.

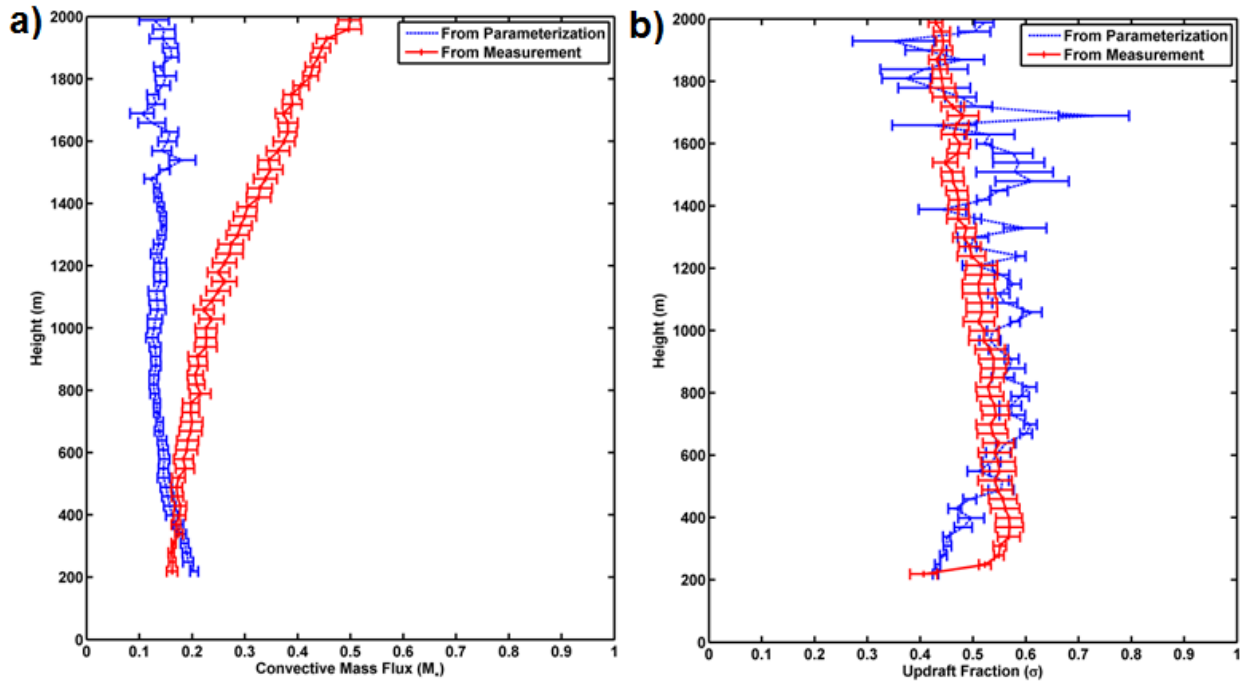


Figure 7: Comparison of parameterized (blue line) and measured values (red line) during the disturbed phase. (a) Convective mass flux and (b) Updraft fraction. The error bars indicate uncertainty in the estimate.

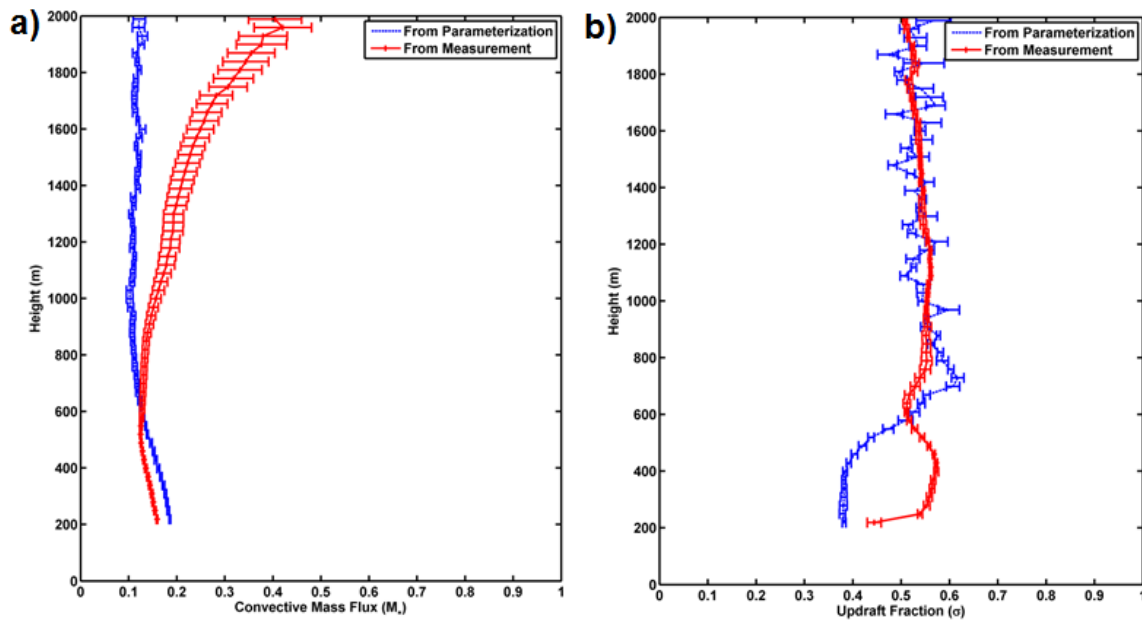


Figure 8: Comparison of parameterized (blue line) and measured values (red line) during the MJO phase. (a) Convective mass flux and (b) Updraft fraction. The error bars indicate uncertainty in the estimate.

Characterization of Precipitation Driven Outflows

As introduced earlier, HRDL was used to track the arrival of precipitation driven outflows as they approached the ship in both the aerosol backscatter intensity and radial velocity data fields. Figure 9 shows an outflow captured by horizontal scans of HRDL as it propagates towards and then passes over

the ship (located in the center). The individual red dots indicate the location of the front during repeated scans – roughly once every ten minutes. The gust increases the lidar backscatter, perhaps because the winds pick up and loft salt and aerosol particles into the boundary layer, where they scatter the lidar beam. By tracking the features through a sequence of scans similar to those in Figure 9 the speed and direction of propagation of the outflow is determined relative to the mean wind and its depth. During legs 2 & 3 this technique was used to identify 220 outflow features.

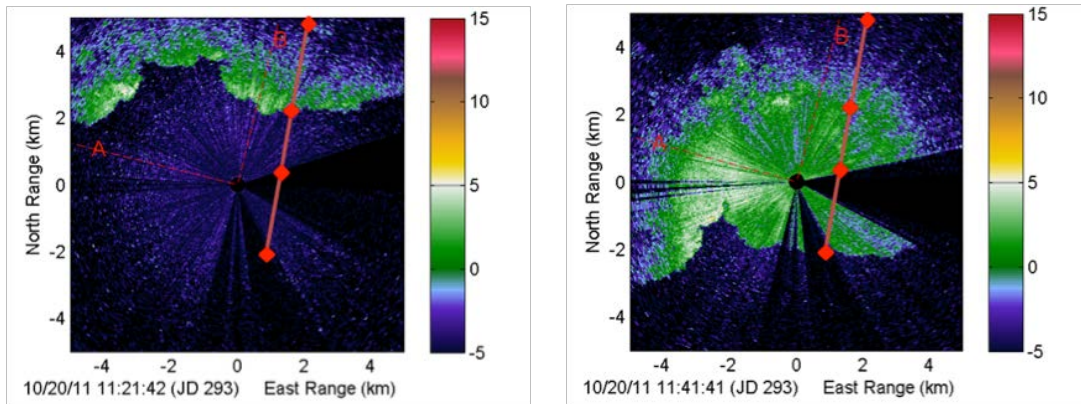


Figure 9: Surface aerosol backscatter from horizontal scans with edge tracking results (in red). These two scans, separated by 20 minutes in time, show the propagation of the leading edge of the outflow.

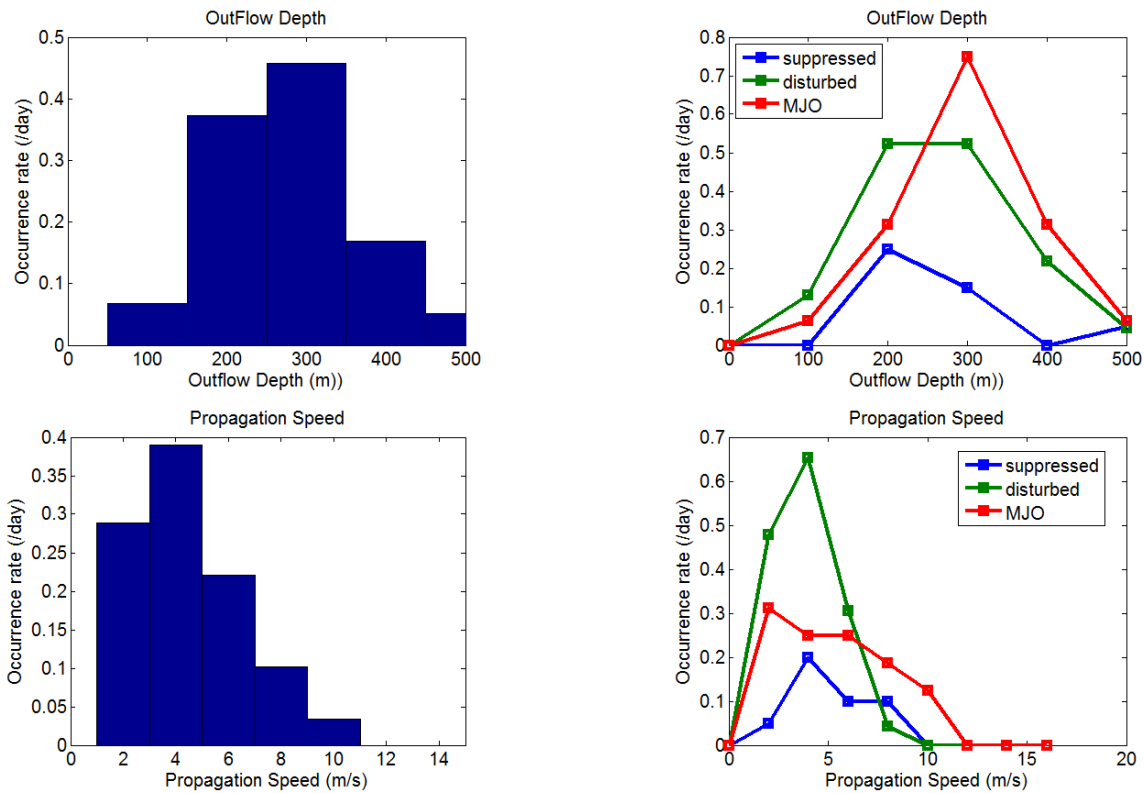


Figure 10: Distribution of outflow depth (top) and propagation speed (bottom) for all common outflows (left) and for different regimes of convection (right).

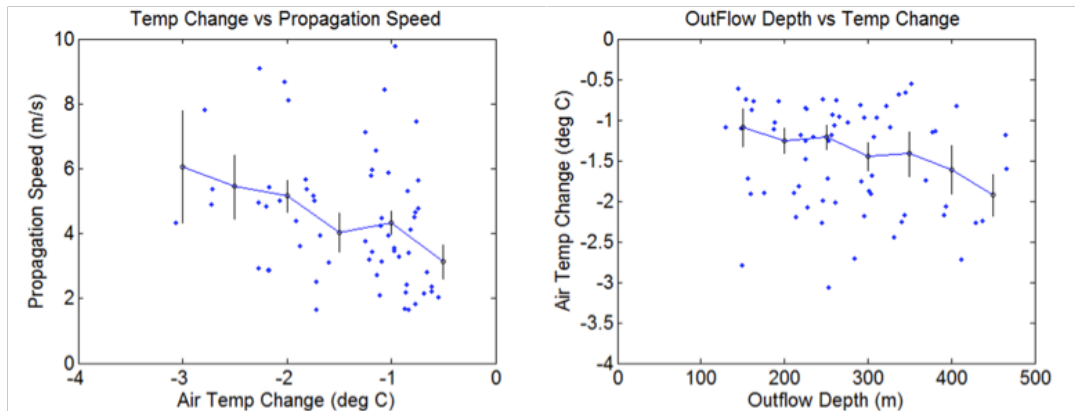


Figure 11: Two plots relating the change in air temperature to the propagation speed and depth of 69 outflows sampled during legs 2&3 of the DYNAMO cruise. The error bars represent a 2 sigma standard deviation of the mean.

In an initial analysis, we identified 69 outflows that were common to both in-situ temperature measurements and lidar analysis (arrival times agreed to within 10 minutes). Using this common set of outflows, Figure 10 shows the distribution of depth and propagation speed for all common outflows (left) and broken out for the different regimes of convection. Outflow Depths between 200 and 300m were most common and propagation speeds of 3-4 m/s relative to the mean wind were most prevalent. Figure 11 shows the relationship between the air temperature drop with outflow passage and the depth and propagation speed of the outflow. Larger temperature changes were associated with faster propagating and deeper outflows.

IMPACT/APPLICATIONS

This work is being done to improve the representation of the Madden-Julian Oscillation (MJO) in global models. It combines remote sensing and in-situ observations made from the RV-Revell during legs 2 & 3 of the DYNAMO experiment to understand processes that govern vertical transport of moisture through the boundary layer and impact the initiation phase of the MJO.

RELATED PROJECTS

The work to measure the mass flux was done with Chris Fairall and Christopher Williams from the NOAA's Earth System research Laboratory and the University of Colorado (CIRES) who helped analyze the w-band radar data, apply the Pinsky retrieval algorithm to remove the impact of the drop fall velocity, and combine them with the lidar data to provide continuous profiles of atmospheric dynamics through the depth of the marine atmospheric boundary layer and to evaluate the model parametrizations. We worked with Paquita Zuidema from the University of Miami, Simon de Szoeke from Oregon State University and Steve Krueger from the University of Utah to identify cold pools encountered by the RV Revelle and on Gan Island and combine this data set with a modelling effort to study how they impact the vertical transport of moisture through the marine atmospheric boundary layer and the subsequent transition from shallow to deep convection observed during the initiation phase of the MJO.

REFERENCES

- Pinsky M., et al. (2010):** Investigation of the turbulent structure of a cloud capped mixed layer using Doppler radar. *Journal of Applied Meteorology and Climatology*, **49**, 1170-1190.
- Lappen C.L., Randall D.A. (2001):** Toward a unified parameterization of the boundary layer moist convection. Part I: A new type of mass flux model. *Journal of atmospheric sciences*, **58**(15), 2021-2036.

PUBLICATIONS

- Brewer, Wm A, C. Fairall, S de Szoeki, P. Zuidema, R. J. Alvarez, A. M. Weickmann, S. P. Sandberg, A. Choukulkar, M Hardesty:** Statistics of Tropical Atmospheric Cold Pool Structure and Occurrence as Sampled by a Scanning Doppler Lidar and In-situ Sensors Aboard the RV Revelle during the Dynamics of the Madden Julian Oscillation (DYNAMO) Experiment, 2013 December *AGU Fall Meeting*, San Fransisco, CA.
- Choukulkar, A, W.A. Brewer, C. Williams, A.A. Grachev, C. W. Fairall:** Ship-based Observations of Turbulence and Mass Flux Transport in the Indian Ocean from the DYNAMO Field Program. 2013 December *AGU Fall Meeting*, San Fransisco, CA.